Acta Oceanol. Sin., 2017, Vol. 36, No. 6, P. 12–22
DOI: 10.1007/s13131-017-0998-y
http://www.hyxb.org.cn
E-mail: hyxbe@263.net

Coupled carbon and sulfur isotope behaviors and other geochemical perspectives into marine methane seepage

LIU Lihua[1]*, FU Shaoying[2], ZHANG Mei[1], GUAN Hongxiang[1], WU Nengyou[3, 4]

[1] Key Laboratory of Gas Hydrate, Guangzhou Institute of Energy Conversion, Chinese Academy of Sciences, Guangzhou 510640, China

[2] Guangzhou Marine Geological Survey, Guangzhou 510760, China

[3] The Key Laboratory of Gas Hydrate of Ministry of Land and Resources, Qingdao Institute of Marine Geology, Qingdao 266071, China

[4] Laboratory for Marine Mineral Resources, Qingdao National Laboratory for Marine Science and Technology, Qingdao 266071, China

Received 12 April 2016; accepted 27 September 2016

Abstract

Methane seepage is the signal of the deep hydrocarbon reservoir. The determination of seepage is significant to the exploration of petroleum, gas and gas hydrate. The seepage habits microbial and macrofaunal life which is fueled by the hydrocarbons, the metabolic byproducts facilitate the precipitation of authigenic minerals. The study of methane seepage is also important to understand the oceanographic condition and local ecosystem. The seepage could be active or quiescent at different times. The geophysical surveys and the geochemical determinations reveal the existence of seepage. Among these methods, only geochemical determination could expose message of the dormant seepages. The active seepage demonstrates high porewater methane concentration with rapid SO_4^{2-} depleted, low H_2S and dissolved inorganic carbon (DIC), higher rates of sulfate reduction (SR) and anaerobic oxidation of methane (AOM). The quiescent seepage typically develops authigenic carbonates with specific biomarkers, with extremely depleted ^{13}C in gas, DIC and carbonates and with enriched ^{34}S sulfate and depleted ^{34}S pyrite. The origin of methane, minerals precipitation, the scenario of seepage and the possible method of immigration could be determined by the integration of solutes concentration, mineral composition and isotopic fractionation of carbon, sulfur. Numerical models with the integrated results provide useful insight into the nature and intensity of methane seepage occurring in the sediment and paleo-oceanographic conditions. Unfortunately, the intensive investigation of a specific area with dormant seep is still limit. Most seepage and modeling studies are site-specific and little attempt has been made to extrapolate the results to larger scales. Further research is thus needed to foster our understanding of the methane seepage.

Key words: marine seepage, authigenic minerals, carbon isotopes, sulfur isotopes, numerical simulation

Citation: Liu Lihua, Fu Shaoying, Zhang Mei, Guan Hongxiang, Wu Nengyou. 2017. Coupled carbon and sulfur isotope behaviors and other geochemical perspectives into marine methane seepage. Acta Oceanologica Sinica, 36(6): 12–22, doi: 10.1007/s13131-017-0998-y

1 Introduction of marine methane seepage

Marine seepage is formed by the release of deep pressurized pore fluids and considered to be a signal pointing directly to deep hydrocarbon reservoirs. Seep occurs at nm to 3 000 m depth of between a few meters and several kilometers. Escaped gaseous and aqueous hydrocarbons mostly methane supports overlain microbial communities. The metabolic byproducts of microorganisms facilitate the precipitation of authigenic minerals, the minerals provide solid substrates for habitation of macrofaunal organisms (Formolo and Lyons, 2013; Grupe et al., 2015). The macrofaunal activities enhance solute transport and influence the redox zonation of sediments through irrigation and geochemical reactions (Hutchens et al., 2010; Meile et al., 2001). The upwelling flow, the micro- and macro-communities and the solid minerals form a unique ecosystem of methane seepage. This ecosystem and the biogeochemical relationships drive the cycling of carbon, sulfur and other elements. The investigation of seepage is thus an elegant approach to study the local element cycle, to trace the paleoceanographic conditions and guide offshore exploration for hydrocarbon deposits (Judd et al., 2002).

Methane seeps occur where the overpressured fluids rise to the sediment surface through cracks and fissures accompanied sometimes by visible evidences. The most obvious evidence is gas flares. The flares could be identified by observation and multi-beam sonar system (Hovland et al., 2012; Jensen et al., 2002; Judd et al., 2002; Martens et al., 1999). Pockmarks and mud volcanos is another identification (Hovland et al., 2012; Nelson et al., 1979) and could be recognized by the high-resolution multi-beam systems and echo sounder electro-magnetic methods (Hovland et al., 2012; Judd et al., 2002; Röemer et al., 2012; Taluk-

Foundation item: The National Natural Science Foundation of China under contract No. 41376076; the Natural Science Foundation of Guangdong Province under contract No. 2015A030313718; the Scientific Cooperative Project by China National Petroleum Corporation and Chinese Academy of Sciences under contract No. 2015A-4813; the National Marine Geological Project, China Geological Survey under contract No. GZH2012006003.
*Corresponding author, E-mail: liulh@ms.giec.ac.cn

der et al., 2013). Microbial mats, seep-related chemosynthetic animals and authigenic minerals are also visible signals of seeps (Barry et al., 1997; Boetius and Suess, 2004; Feng et al., 2015; Hovland et al., 2012; Joye et al., 2010; Knittel et al., 2005). Above visual quantifications could be revealed by remotely operated vehicle (ROV), by seismic and hydroacoustic surveys (Regnier et al., 2011; Röemer et al., 2012; Talukder et al., 2013).

Worldwide scientists have investigated prospective areas of methane seeps during the past decades (Foucher et al., 2009; Han et al., 2013; Paull et al., 2008; Rollet et al., 2006; Yin et al., 2003). The investigation suggests that methane seeps have been reported from (1) every see and ocean; (2) a broad range of oceanographic settings from the coast to the deep ocean; (3) a wide variety of geological environments (Judd, 2003).

2 Geochemical properties of marine methane seepage

Geochemical properties indicate the seepage especially suitable for the dormant and ancient seepage. High concentrations of methane, even higher than saturated concentration have been determined in many seeping areas (Archer, 2007; Huang et al., 2008; Lim et al., 2011). The high concentration fuels the geochemical reactions and accompanied by a specific isotopic distribution. The coupled processes of geochemical reactions and microorganism activities form the metabolic foundation of marine seeps. The seeps could be revealed by the composition of minerals, the distribution of solutes and isotopic fractionations of elements (Joye et al., 2010; Treude et al., 2007). Dormant or ancient seepage may only be delineated by geochemical signals, e.g., authigenic mineral, solutes distribution, ionic and stable isotopic composition (Bayon et al., 2007; Cook et al., 2011; Feng and Chen, 2015; Han et al., 2008; Malone et al., 2002; van Dongen et al., 2007).

2.1 *Authigenic minerals*

The presence of authigenic minerals and mineral aggregates indicates a high upwelling flux and the active of microorganism. Among the authigenic minerals, carbonate is the commonest one and has been well investigated (Bouloubassi et al., 2006; Gieskes et al., 2005; Greinert et al., 2002; Luff et al., 2005). The carbonates are mainly aragonite, Mg-calcite and (proto)-dolomite, also Fe- and Mn-carbonates (Haas et al., 2010; Han et al., 2008). Various carbonates appear under different geochemical conditions and the formation of carbonates is mediated by the activities of microorganism (Han et al., 2014; Liebetrau et al., 2014). Other authigenic minerals, e.g., pyrite (FeS_2), gypsum ($CaSO_4{\cdot}2H_2O$), barite ($BaSO_4$) and greigite (Fe_3S_4) have also been reported (Greinert et al., 2001; Joye et al., 2010; Lin et al., 2016a, c ; Peckmann et al., 2001; Sassen et al., 2004; van Dongen et al., 2007; Vanneste et al., 2013). The association of carbonates with gas emissions and populations of chemosynthetic faunas has been a widely used criterion to identify the hydrocarbon seeps (Feng and Chen, 2015; Feng et al., 2015; Suess, 2014).

2.2 *Distribution of solutes in interstitial water*

The distribution of solutes in interstitial water may directly point the seepage. Methane seepages typically harbor communities of micro- and macro-organism, which mediates the anaerobic oxidation of methane (AOM) to produce HCO_3^- and HS^-. HCO_3^- is the main part of dissolved inorganic carbon (DIC=$[CO_3^{2-}]$+$[HCO_3^-]$+$[CO_2]$+$[H_2CO_3]$) which could precipitate with metallic ion as carbonate. In the active seep site, porewater CH_4 and dissolved organic carbon (DOC) concentrations are thus high with significant NH_4^+, rapid SO_4^{2-} depleted, low H_2S and DIC, higher rates of sulfate reduction (SR) and AOM (Knittel and Boetius, 2009; Treude et al., 2005). The high rates of methaneogenesis are associated with either abundant natural gas or deep hydrocarbon reservoir. The high methanotrophic rate is accompanied by the high DIC and the recrystallization of carbonates (Boetius et al., 2000; Knittel and Boetius, 2009). The depth of sulfate-methane reaction zone reveals the intensity of upwelling flux (Chuang et al., 2013; Lin et al., 2016c; Luff and Wallmann, 2003). For the inactive or quiescent seepages the distribution of solutes provide limit signal with the geological time (Haeckel et al., 2004). Only carbonate and isotopic fractionations of elements preserve more messages (Ge et al., 2015; Novikova et al., 2015). Some models have been used to quantitatively describe the seepage and the model work will be introduced below (Liu et al., 2016a; Luff et al., 2004; Wallmann et al., 2006).

2.3 *Stable isotopic fractionation*

The stable isotopes and biomarkers have been the advanced criteria for recognizing ancient seeps (Bohrmann et al., 1998; Feng et al., 2015; Formolo and Lyons, 2013; Gieskes et al., 2005; Hu et al., 2015; Lin et al., 2016c; Lu et al., 2015; Sivan et al., 2007). The fractionation of element isotopes during uptake and metabolism of methanogens and methanotrophy is controlled primarily by the source material and kinetic isotope effects (Feng et al., 2015; Novikova et al., 2015; Whiticar, 1999).

2.3.1 *Stable isotope of carbon*

(1) Methane gas

Except for methane, hydrogen sulfide and carbon dioxide has been determined in headspace (Himmler et al., 2015; Joye et al., 2010; Kastner et al., 1998; Malone et al., 2002; Suess, 2005). However, only a few sites reported isotopic composition of methane and hydrogen sulfide. The reported gaseous $\delta^{13}C$ were listed in Tables 1 and 2 (for sulfide) and marked in Figs 1 and 2 (for sulfide).

Biogenic methane gas commonly shows an extremely negative $\delta^{13}C$ value of –110‰ to –50‰ and the thermogenic methane is generally, but not exclusively, enriched in ^{13}C (>–50‰), the mixture located in the transition region (Joye et al., 2010; Whiticar, 1999).

(2) Dissolved inorganic carbon (DIC)

The $\delta^{13}C$ in DIC has been widely investigated. The values were listed in Table 1 and shown in Fig. 1. Normal $\delta^{13}C_{DIC}$ value of ocean water is around 2‰ (Faure, 1986). The anaerobic oxidation of methane with medium of microorganism will obtain low $\delta^{13}C$ of around –20‰ to –50‰ (Hu et al., 2015; Kastner et al., 1998; Lin et al., 2001; Malone et al., 2002; Martens et al., 1999; Roalkvam et al., 2011). Generally, $\delta^{13}C$ values of DIC are higher than gaseous methane in a certain sites since the lightest fraction could preferentially escape to gaseous or react.

However, in the inactive seepages, both the distribution of solutes and the isotopic data provide limit message, further information have to recur the signature of solid carbonates.

(3) Authigenic carbonate

A direct consequence of methane consumption is the precipitation of carbonates with depleted ^{13}C (Grupe et al., 2015; Magalhães et al., 2012). The values in remnant bacterial mats could be –81.6‰ (Novikova et al., 2015). Some $\delta^{13}C$ of the carbonates are listed in Table 1. Most seepage carbonates show a higher $\delta^{13}C$ than gaseous methane and similar to that of DIC (Aloisi et al., 2004; Berndt et al., 2014; Cook et al., 2011; Feng and Chen, 2015; Formolo and Lyons, 2013; Formolo et al., 2004; Himmler et al., 2015; Malone et al., 2002; Treude et al., 2005;

Table 1. Isotopic value of carbon $\delta^{13}C$ in gas, liquid and solid phases

	Value/‰	Mechanism	Reference and locality
$\delta^{13}C$ (methane gas)	–110––60	Reduction of CO_2→CH_4	Kastner et al. (1998)
			Cascadia subduction zone
	–110––50	biogenic CH_4	Whiticar (1999)
	–50––20	thermogenic CH_4	Gulf of Mexico
	–88–	methanogenesis at deepwater sites	Joye et al. (2010)
	–54–62	mixed thermogenic and biogenic origin	northern Gulf of Mexico
	–67.5––64.5	with dissociated gas hydrate	
	–88.3––54.48	biogenic formation at the deep sites	Martens et al. (1999)
			Eckernforde Bay
	–70.3––66.7	seeps	Himmler et al. (2015)
			Makran convergent margin
$\delta^{13}C$ (DIC)	–49.0––47.1	derived from AOM by microorganisms	Roalkvam et al. (2011)
			Nyegga area
	–38.1––1.3	organoclast sulfate reduction and AOM	Hu et al. (2015)
			Northeast of Dongsha, SCS
	–35––6	CH_4 advection into the sulfate reduction zone	Kastner et al. (1998)
			Cascadia subduction zone
	–27––12	CH_4 oxidized or vented from shelf sediments	Malone et al. (2002)
			outer New Jersey shelf
	–21	sulfate reduction by AOM	Lin et al. (2001)
			Southwest Africa margin
	2	dissolution (+)/precipitation (–)	Faure (1986)
	–15.5–19.66	AOM active area	Martens et al. (1999)
			Eckernforde Bay
$\delta^{13}C$ (solid minerals)	–81.6––76.9	remnant bacterial mats	Novikova et al. (2015)
	–46.5––33	biogenic methane-derived carbonate	ancient cold seep, Black Sea
	–61	methane-derived authigenic carbonates	Grupe et al. (2015)
			Southwest African continental margin
	–56.2––8.4	methane-derived authigenic carbonates	Magalhães et al. (2012)
			Gulf of Cadiz
	–55.3––34.3	authigenic carbonate	Feng and Chen (2015)
			Formosa ridge, South China Sea
	–54.6––39.8	seep within oxygen minimum zone	Himmler et al. (2015)
	–54.3––48.8	seep from non-oxygen minimum zone	Makran convergent margin
	–48.7±2.7	Mg-calcite	Elvert et al. (2000)
	–45.4±3.7	Mg-calcite/aragonite	cold seep eastern Aleutian
	–41.4––27.1	methane related authigenic carbonate	Berndt et al. (2014)
			seepage off Svalbard
	–47.8––26.8	methane-derived carbonate	Lu et al. (2015)
			Shenhu Area, SCS
	–30––20	multiple carbon source carbonate	Southwest Taiwan
	–37	bulk carbonate	Bayon et al. (2007)
	0–29	down-core profile	Niger Delta, hydrate zone, pockmark area
	–41.7	calcite	Malone et al. (2002)
	–17.67––16.4	siderite	Outer New Jersey shelf
	–16.4–8.8	dolomite cement	
	–38.91–0.99	wide range of carbon source	Formolo et al. (2004)
			cold seep in Gulf of Mexico
	–28.9––24.8	carbon crust sediment water interface	Aloisi et al. (2004)
			eastern Mediterranean Sea
	–24.6	carbon crusts	Treude et al. (2005)
			Chilean Margin
	–24.1––22.4	authigenic carbon	Cook et al. (2011)
	–17––2	*N. pachyderma* Planktic foraminifer	Southeast Bering Sea
	–6.8–1	*U. peregrine* Benthic foraminifer	
	–19.8––2.1	microbially induced carbonate	Formolo and Lyons (2013)
			Gulf of Mexico

to be continued

Continued from Table 1

	Value/‰	Mechanism	Reference and locality
	–3.0–-0.5	benthic foraminifera with hydrate dissociation	Wang et al. (2013) Baiyun Sag
δ^{13}C (biomark)	–140.8–-105.7	Pentamethylicosane (PMI)	Ge et al. (2015) Northern South China Sea
	–139–-123	Pentamethylicosane (PMI)	Guan et al. (2013) Northern South China Sea
	–130.3–-93.5	C_{20} and C_{25} isoprenoid	Elvert et al. (2000)
	–74.4–-60.5	squalene and diploptene	cold seep eastern Aleutian subduction zone
	–127–85	crocetane and PMI	Himmler et al. (2015) Makran convergent margin
	–101–-79	general unidentified hydrocarbons	Peckmann and Thiel (2004)
	–28–32	n-alkanes from iron sulfide nodules	van Dongen et al. (2007) Pliocene Valle Ricca
	–79–-72	archaeol	Cook et al. (2011)
	–60–-42	di-anteiso C_{15}-glyceroldiether (DAGE-C_{30})	Southeast Bering Sea
	–35–-30	n-alcohols	
	–25–-22	isololiolide & ioliolide	
	–22	biphytane	
	–58–-26	monocyclic & acyclic biphytane	
	–20	bicyclic & tricyclic biphytane & cren (different at different layer and depth)	

Wang et al., 2013). This scheme may be due to the fractionation during evaporation and metabolism. Cold-seep carbonates are characterized by a negative δ^{13}C value, most are between 0‰ to –40‰ or even lower (Tong et al., 2013), and the lowest one was –61‰ in the Southwest African continental margin (Grupe et al., 2015). This value clearly indicates the methane derived carbonates. A high value of 0‰–29‰ was determined in a down core profile in a pockmark area of Niger Delta (Bayon et al., 2007) which could be a geothermal or non-methane driven source.

(4) Biomarkers

Abundant fossilized microbes are preserved in seep carbonates (Cook et al., 2011; Elvert et al., 2000; Guan et al., 2016; Han et al., 2008; Peckmann and Thiel, 2004). Fossilized biomarkers could be extracted with distinctive carbonate fabrics and stable isotope signatures. The extractants could reveal the biogeochemical route and environmental conditions of ancient seep sites. The oldest biomarker recorded in the 300-million-year-old limestone (Birgel et al., 2008; Suess, 2014). The characteristic biomarkers in ancient seep environments are ^{13}C-depleted archaeal isoprenoids, linear and methyl-branched carbon skeletons and hopanoids of bacterial origin (Peckmann and Thiel, 2004). Beyond above species, a wide range of biomarkers, including fatty acids, isoprenoidal and non-isoprenoidal ether lipids and hopanoids have also been determined in cold seeps (Pancost et al., 2001; Schouten et al., 1998; Stadnitskaia et al., 2003, 2005; van Dongen et al., 2007). Above biomarkers are greatly depleted ^{13}C (–40‰ to –140‰), the lightest could be lower than –140.8‰ in a cold seep from the northern South China Sea (Ge et al., 2015). A high value of 32‰ for n-alkanes from iron sulfide nodules (saturated hydrocarbon) could be due to the non-methane source. However, extreme variability over narrow spatial and temporal scales within short distances (m) is common for active and dormant seeps (Formolo and Lyons, 2013; Li et al., 2007).

2.3.2 *Stable isotope of sulfur*

Isotopic fractionation of sulfur suggests the existence and evolution of seepage because both the degradation of organic carbon and AOM are accompanied by microbial sulfate reduction (Boudreau, 1996; Lin et al., 2016a, b ; Luff et al., 2000). Microorganisms have long been known to fractionate isotopes during their sulfur metabolism. Both ^{34}S and ^{18}O which will be introduced next have been used as indicators of the origin and geochemical routine of seep site (Aharon and Fu, 2000, 2003; Faure, 1986; Feng et al., 2015; Formolo and Lyons, 2013; Kastner et al., 1998).

Some of the published δ^{34}S values were listed in Table 2 and Fig. 2. A few values reported gaseous sulfur and hydrogen sulfide and substantial liquid phase, and sulfate in porewater. The extreme high or low value of isotopic fraction appears in the reactive area which indicates the seepage. The range of gaseous hydrogen sulfide was –20‰ to 25‰ depending on the local formation, sulfur source and metabolic processes. Most dissolved sulfate in pore water have δ^{34}S value similar to seawater which is about 20‰ and the maximum could be 70.8‰ in the intensive sulfate reduction area in the Gulf of Mexico (Aharon and Fu, 2003). Pyrite, typically occurring as a framboidal crystal aggregate is the most common non-carbonate mineral in methane seep (Lin et al., 2016b; Peckmann and Thiel, 2004) another one is gypsum (Lin et al., 2016a). Figure 2 and Table 2 show clearly that $\delta^{34}S_{pyrite}$ cover a broad range of 47‰ to –45‰ (Lin et al., 2016a; Peckmann and Thiel, 2004) which indicated the complex source and synthesis of pyrite. Most solid phase including pyrite, total reduced inorganic sulfur and acid volatile sulfur. Elemental sulfur obtained light sulfur mainly around 0‰ to –20‰. However, the different among various solid phases is only the extraction method. The mechanism of the formation and fractionation is still unclear, further research is needed.

2.3.3 *Stable isotope of oxygen*

The δ^{18}O values were reported for carbonate, gypsum, sulfate and interstitial water samples. The determination of ^{18}O in seepage is limit and scattered, the data are listed in Table 3 (Aharon

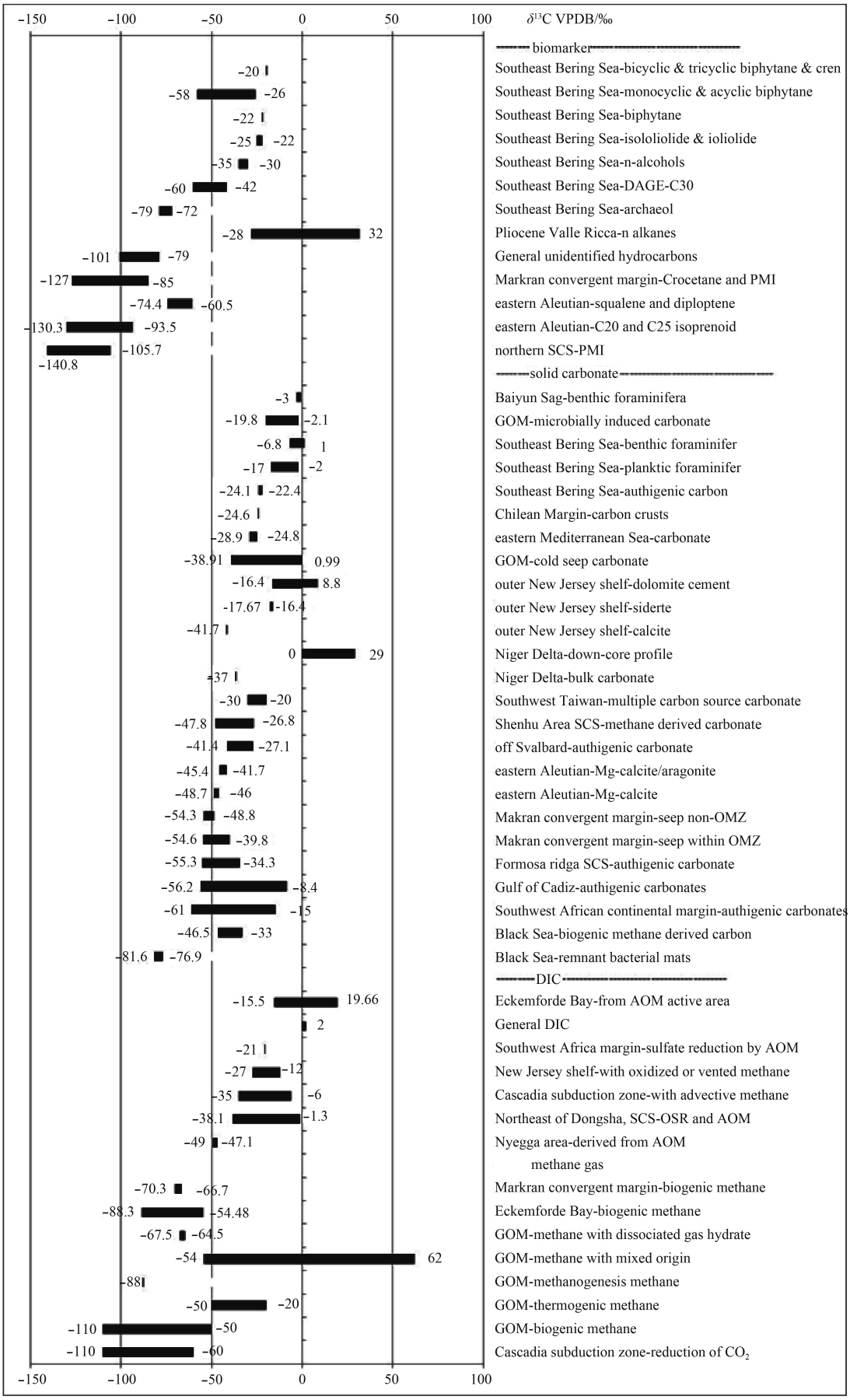

Fig. 1. The distribution of $\delta^{13}C$ in various phases.

Table 2. Isotopic value of sulfate $\delta^{34}S$ in various phases

	Value/‰	Mechanism	Reference and locality
$\delta^{34}S$-H_2S (gas)	–20.8–-20.0	intermediate reactive site	Formolo and Lyons (2013)
	–19.7	highly reactive site	hydrate and hydrocarbon rich seep, Gulf of Mexico
	12.4±5.4	in a core from a tube worm setting coexisting H_2S	Aharon and Fu (2003) northern Gulf of Mexico
	22	sulfide	Kastner et al. (1998)
	27.4	while gas hydrate dissociated	Cascadia subduction zone
	2.3–25.8	sulfide in pore fluids	Aharon and Fu (2003) Gulf of Mexico
$\delta^{34}S$-SO_4 (liquid)	20–20.3	sea water	Kastner et al. (1998), Faure (1986)
	60	in intense sulfate reduction zone	Kastner et al. (1998) Baltic Sea
	20.7–23.4	sulfate in pore fluids increase with depth	Aharon and Fu (2000) Gulf of Mexico
	–23.6	sulfate in the pore fluids from seep sediments	
	29.8	sulfate in a core from a tube worm setting	Aharon and Fu (2003) Gulf of Mexico
	20.7–70.8	sulfate in pore fluids	
	32.2–50.9	sulfate in pore fluids	
	19.8–20.1	background site	Formolo and Lyons (2013)
	19.9–20.2	non-reactive site	hydrate and hydrocarbon rich
	23.4–26.3	intermediate reactive site	seep, Gulf of Mexico
	–54.1	highly reactive site	
$\delta^{34}S$ (solid)	$\delta^{18}S_{Pyrite}$ –45.4–-10.8	sulfate-methane transition zone	Lin et al. (2016c) hydrate-bearing region, SCS
	$\delta^{18}S_{Pyrite}$ –41–47	seep associated pyrite to metabolism of SRB	Peckmann and Thiel (2004)
	$\delta^{18}S_{Pyrite}$ –37.6–37.9	seep site	Lin et al. (2016a)
	$\delta^{18}S_{gypsum}$ –24.5–0.9		Shenhu Area, SCS
	$\delta^{18}S_{Pyrite}$ –41.6–114.8	seep site	Lin et al. (2016b)
	$\delta^{18}S_{Pyrite}$ –35.0	oxygenated ocean with less pyrite burial	Sahoo et al. (2012) Doushantuo Formation
	$\delta^{18}S_{TRIS}$ –24.9–-5.2	bacterial SO_4^{2-} reduction	Formolo et al. (2004)
	$\delta^{18}S_{Pyrite}$ –19.2–-11.9	intermediate reactive site	cold seep in Gulf of Mexico
	$\delta^{18}S_{acid\ volatile\ sulfur}$ –25.7–-20.6		
	$\delta^{18}S_{elemental\ sulfur}$ –23.6–-6.8		
	$\delta^{18}S$ S_{Pyrite} –21.3–-7.8	highly reactive site	Formolo and Lyons (2013)
	$\delta^{18}S_{acid\ volatile\ sulfur}$ –10.4–11.9		hydrate and hydrocarbon rich
	$\delta^{18}S_{elemental\ sulfur}$ –3.3–18.3		seep, Gulf of Mexico

and Fu, 2000; Aharon et al., 1992; Davidson et al., 1978; Faure, 1986; Feng and Chen, 2015; Himmler et al., 2015; Kastner et al., 1998; Malone et al., 2002; Matsumoto, 2000; Novikova et al., 2015; Tong et al., 2013). Most carbonate $\delta^{18}O$ lies between 0‰–10‰, only the cold seep area in the Gulf of Mexico shows a high value of 35.33‰ (Formolo et al., 2004). One reported $\delta^{18}O$ in gypsum was 5.3‰–12.3‰ in the Shenhu Area, SCS (Lin et al., 2016c). The mineralogy of the authigenic minerals and the source of fluid is probably the main influence on the $\delta^{18}O$ (Cook et al., 2011). Two interstitial water samples were around zero, and the samples in active area showed a higher level. The high level could be more than 20‰ which may due to the lighter portion preferentially enter the gaseous phase (Aharon and Fu, 2000).

3 Episodes of methane seepage

The methane seepage in one site may spurt several times over geologic time. Several layers of methane-derived carbonates are direct evidence of the episode (Magalhães et al., 2012). The episode could be determined by the age of carbonates and paleo-environmental condition. The seep carbonates with a series of consecutive U/Th dating has been reported in the northern South China Sea which established the periods of seep events (Feng and Chen, 2015; Han et al., 2014). Different lithologic groups evidenced the extensive episodes (Magalhães et al., 2012) and the fluctuation of depleted $\delta^{13}C$ record several leaching events during glacial intervals (Hyun et al., 2014). If the sulfate methane transition zone is deep in the seafloor, the authigenic carbonates formed much older than the episode of methane flux (Cook et al., 2011; Novikova et al., 2015). Periodic, catastrophic release of stored methane in gas hydrates implicated also climate change scenarios (Dickens et al., 1995; Hyun et al., 2014; Ménot and Bard, 2010). However, the seep activity is also affected by tidal, sea level, climate change and orbital. Detailed investigation is needed to identify the episode and causes of seepage.

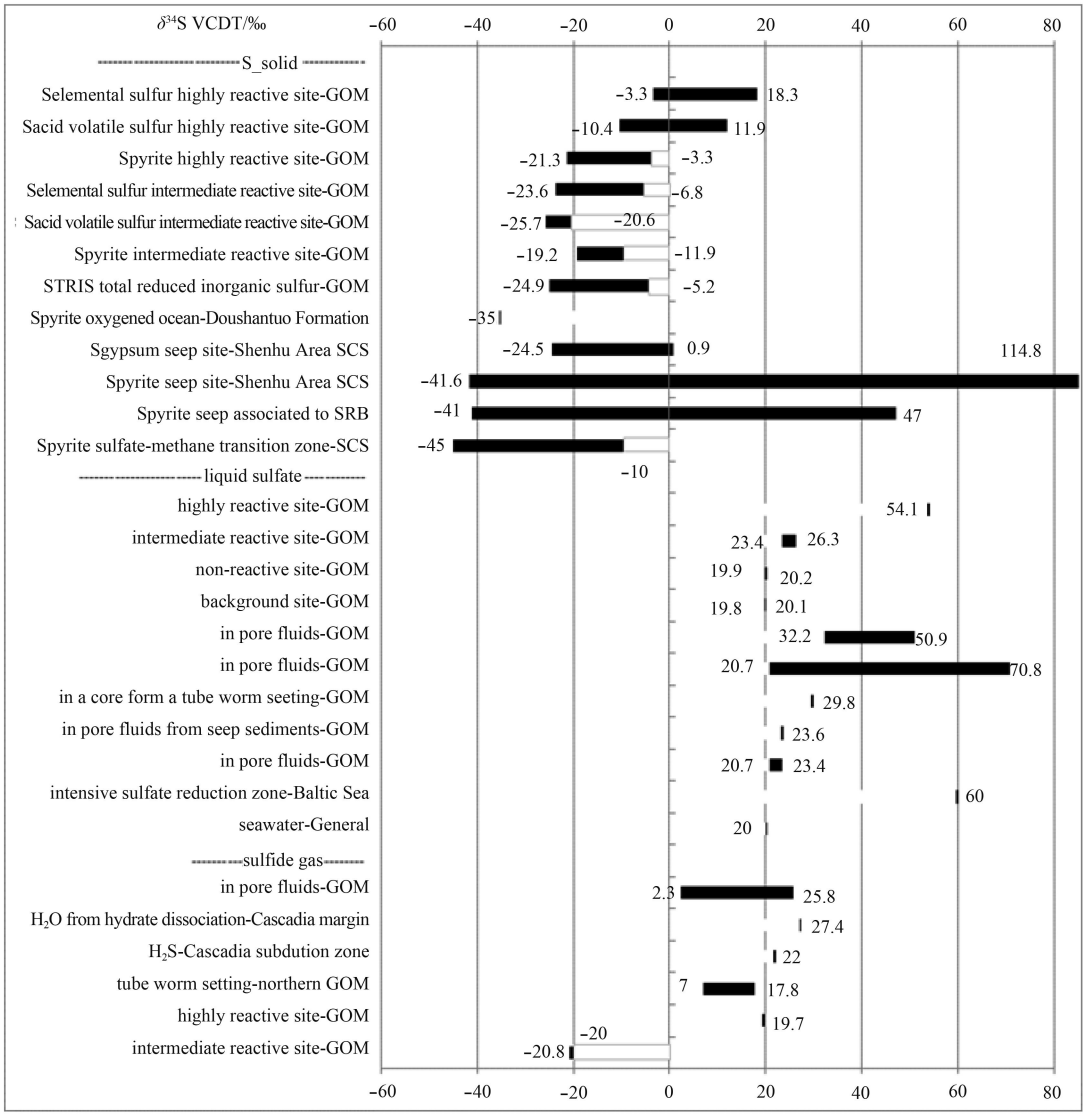

Fig. 2. The distribution of $\delta^{34}S$ in various phases.

4 Numerical simulation of the seepage

Simulation tools have greatly improved our quantitative understanding of seepage and help us to reconstruct the environmental conditions in marine sediments. The processes from methaneogenesis to methantrophy have been extensively modeled (Aloisi et al., 2004; Arning et al., 2011; Meysman et al., 2003; Reed et al., 2011; Scholz et al., 2011). The benthic fluxes of dissolved inorganic carbon (DIC) and alkalinity (TA) and carbonate deposition has been estimated from coastal sediments (Boudreau, 1996; Krumins et al., 2013; Luff et al., 2000, 2005). Currently simulations could define the path of geochemical reactions and mineralization and evaluate the kinetic reaction rate (Liu et al., 2016b). However, the knowledge about the episode and the cycle of seepage is still limit and further research is necessary.

5 Conclusions

For the exploration of hydrocarbon reservoir, the investigation of seepage is an elegant method. The study of seepage contributes also to the reconstruction of paleoceanographic and environmental conditions. During the past decades, we got some knowledge about methane source, methane reaction, consumption and the episodes of seep. Generally, the survey of seepage starts from the geophysical reconnaissance to the geochemical determination. The geochemical determination, e.g., methane gas, DIC, carbonates and biomarkers could be used to evaluate the geological background, the geochemical reactions and the mechanism of compound immigration. The seepage could be active or dormant and the geochemical prospection is a suitable approach especially for the dormant seepage. Unfortunately, it is impossible to determine the source neither the transport mechanism with one element isotopic ratio or one phase distribution. The combination of carbon, sulfur and oxygen isotope behaviors with other geochemical determination is always necessary. With the integrated field and geochemical determination, model could quantitatively describe the kinetic reactions, the formation of minerals and the flux of seepage. Eventually we may better understand the system, predicate the leaching events and access the climate effect of methane seepage. However, the intensive investigation of a specific area for methane seepage, especially for dormant seep is still limit. Most seepage investigation tends nevertheless to be site-specific since the geological formations are highly variable even between two adjacent cores separated by less than a meter, and little attempt has been made to extrapol-

Table 3. Isotopic value of oxygen $\delta^{18}O$ in liquid and carbonates

	Value/‰	Mechanism	Reference and locality
$\delta^{18}O$ (liquid)	–1.5–-0.5	interstitial water	Malone et al. (2002)
			New Jersey shelf
	–0.5–0.3	interstitial water, hydrate zone	Matsumoto (2000)
			Black Ridge
	–0.15–1	bottom sea water (7–18°C)	Aharon et al. (1992)
			Gulf of Mexico
	1.002 7–1.003 1	ice and water	Davidson et al. (1978)
	2.9	H_2O dissociated gas hydrate	Kastner et al. (1998)
			Cascadia margin
	9.7	modern seawater	Faure (1986)
	10.5–12.1	sulfate in pore fluids	Aharon and Fu (2000)
		increase with depth	Gulf of Mexico
	17.3	sulfate in a core from a tube worm setting	
	11.1–23.6	sulfate in the pore fluids from seep sediments	
$\delta^{18}O$ (carbonate and gypsum)	–0.1–4	with hydrate dissociation	Wang et al. (2013)
			Baiyun Sag
	0.2–1.3	methane-derived carbonate	Novikova et al. (2015)
			ancient cold seep, Black Sea
	1–9	bulk carbonate	Bayon et al. (2007)
	5	authigenic carbonate	Niger Delta
		with hydrate dissociation	
	1.3–6.5	authigenic carbonate	Malone et al. (2002)
			outer New Jersy shelf
	1.4–5.1	authigenic carbonate	Tong et al. (2013)
		with hydrate dissociation	northern South China Sea
	1.3–2.1	seep within oxygen minimum zone	Himmler et al. (2015)
	2.2–4.2	seep non-oxygen minimum zone	Makran convergent margin
	0.1–3.2	highly reactive site, hydrate and	Formolo and Lyons (2013)
		hydrocarbon rich seep	Gulf of Mexico
	3	secondary $CaCO_3$	
	3.4–6.5	authigenic carbonate	Cook et al. (2011)
	3.6–4.8	authigenic carbonate	Feng and Chen (2015)
			Formosa ridge, South China Sea
	5.6	foraminifer	Southeast Bering Sea
	0.8–6.8	methane-derived authigenic	Magalhães et al. (2012)
		carbonates	Gulf of Cadiz
	21.51–35.33	^{18}O enrichment carbonates	Formolo et al. (2004)
			cold seep in Gulf of Mexico
	5.3–12.3	authigenic gypsum	Lin et al. (2016a)
			Shenhu Area, SCS

ate the results to larger scales. Further research is thus needed to foster our understanding of the methane seepage.

References

Aharon P, Fu Baoshun. 2000. Microbial sulfate reduction rates and sulfur and oxygen isotope fractionations at oil and gas seeps in deepwater Gulf of Mexico. Geochimica et Cosmochimica Acta, 64(2): 233–246

Aharon P, Fu Baoshun. 2003. Sulfur and oxygen isotopes of coeval sulfate-sulfide in pore fluids of cold seep sediments with sharp redox gradients. Chemical Geology, 195(1–4): 201–218

Aharon P, Roberts H H, Snelling R. 1992. Submarine venting of brines in the deep gulf of mexico: observations and geochemistry. Geology, 20(6): 483–486

Aloisi G, Wallmann K, Haese R R, et al. 2004. Chemical, biological and hydrological controls on the ^{14}C content of cold seep carbonate crusts: numerical modeling and implications for convection at cold seeps. Chemical Geology, 213(4): 359–383

Archer D. 2007. Methane hydrate stability and anthropogenic climate change. Biogeosciences, 4(4): 521–544

Arning E T, Fu Yunjiao, van Berk W, et al. 2011. Organic carbon remineralisation and complex, early diagenetic solid-aqueous solution-gas interactions: case study ODP Leg 204, Site 1246 (Hydrate Ridge). Marine Chemistry, 126(1–4): 120–131

Barry J P, Kochevar R E, Baxter C H. 1997. The influence of pore-water chemistry and physiology on the distribution of vesicomyid clams at cold seeps in Monterey Bay: implications for patterns of chemosynthetic community organization. Limnology and Oceanography, 42(2): 318–328

Bayon G, Pierre C, Etoubleau J, et al. 2007. Sr/Ca and Mg/Ca ratios in Niger Delta sediments: implications for authigenic carbonate genesis in cold seep environments. Marine Geology, 241(1–4): 93–109

Berndt C, Feseker T, Treude T, et al. 2014. Temporal constraints on hydrate-controlled methane seepage off svalbard. Science, 343(6168): 284–287

Birgel D, Himmler T, Freiwald A, et al. 2008. A new constraint on the

antiquity of anaerobic oxidation of methane: late Pennsylvanian seep limestones from southern Namibia. Geology, 36(7): 543–546

Boetius A, Ravenschlag K, Schubert C J, et al. 2000. A marine microbial consortium apparently mediating anaerobic oxidation of methane. Nature, 407(6804): 623–626

Boetius A, Suess E. 2004. Hydrate ridge: a natural laboratory for the study of microbial life fueled by methane from near-surface gas hydrates. Chemical Geology, 205(3–4): 291–310

Bohrmann G, Greinert J, Suess E, et al. 1998. Authigenic carbonates from the Cascadia subduction zone and their relation to gas hydrate stability. Geology, 26(7): 647–650

Boudreau B P. 1996. A method-of-lines code for carbon and nutrient diagenesis in aquatic sediments. Computers & Geosciences, 22(5): 479–496

Bouloubassi I, Aloisi G, Pancost R D, et al. 2006. Archaeal and bacterial lipids in authigenic carbonate crusts from eastern Mediterranean mud volcanoes. Organic Geochemistry, 37(4): 484–500

Chuang Peichuan, Dale A W, Wallmann K, et al. 2013. Relating sulfate and methane dynamics to geology: accretionary prism offshore SW Taiwan. Geochemistry, Geophysics, Geosystems, 14(7): 2523–2545

Cook M S, Keigwin L D, Birgel D, et al. 2011. Repeated pulses of vertical methane flux recorded in glacial sediments from the southeast Bering Sea. Paleoceanography, 26(2): PA2210

Davidson D W, Garg S K, Ripmeester J A. 1978. NMR behavior of the clathrate hydrate of tetrahydrofuran: II. Deuterium measurements. Journal of Magnetic Resonance (1969), 31(3): 399–410

Dickens G R, O'Neil J R, Rea D K, et al. 1995. Dissociation of oceanic methane hydrate as a cause of the carbon isotope excursion at the end of the paleocene. Paleoceanography, 10(6): 965–971

Elvert M, Suess E, Greinert J, et al. 2000. Archaea mediating anaerobic methane oxidation in deep-sea sediments at cold seeps of the eastern Aleutian subduction zone. Organic Geochemistry, 31(11): 1175–1187

Faure G. 1986. Principles of Isotope Geology. 2nd ed. New York: Wiley

Feng Dong, Chen Duofu. 2015. Authigenic carbonates from an active cold seep of the northern South China Sea: new insights into fluid sources and past seepage activity. Deep Sea Research Part II: Topical Studies in Oceanography, 122: 74–83

Feng Dong, Cheng Ming, Kiel S, et al. 2015. Using *Bathymodiolus* tissue stable carbon, nitrogen and sulfur isotopes to infer biogeochemical process at a cold seep in the South China Sea. Deep Sea Research Part I: Oceanographic Research Papers, 104: 52–59

Formolo M J, Lyons T W. 2013. Sulfur biogeochemistry of cold seeps in the Green Canyon region of the Gulf of Mexico. Geochimica et Cosmochimica Acta, 119: 264–285

Formolo M J, Lyons T W, Zhang Chuanlun, et al. 2004. Quantifying carbon sources in the formation of authigenic carbonates at gas hydrate sites in the Gulf of Mexico. Chemical Geology, 205(3–4): 253–264

Foucher J P, Westbrook G K, Boetius A, et al. 2009. Structure and drivers of cold seep ecosystems. Oceanography, 22(1): 92–109

Ge Lu, Jiang Shaoyong, Blumenberg M, et al. 2015. Lipid biomarkers and their specific carbon isotopic compositions of cold seep carbonates from the South China Sea. Marine and Petroleum Geology, 66: 501–510

Gieskes J, Mahn C, Day S, et al. 2005. A study of the chemistry of pore fluids and authigenic carbonates in methane seep environments: kodiak Trench, Hydrate Ridge, Monterey Bay, and Eel River Basin. Chemical Geology, 220(3–4): 329–345

Greinert J, Bohrmann G, Suess E. 2001. Gas hydrate-associated carbonates and methane-venting at Hydrate Ridge: classification, distribution, and origin of authigenic lithologies. In: Paull C K, Dillon W P, eds. Natural Gas Hydrates: Occurrence, Distribution, and Detection. Washington, DC: American Geophysical Union, 99–113

Greinert J, Bollwerk S M, Derkachev A, et al. 2002. Massive barite deposits and carbonate mineralization in the Derugin Basin, Sea of Okhotsk: precipitation processes at cold seep sites. Earth and Planetary Science Letters, 203(1): 165–180

Grupe B M, Krach M L, Pasulka A L, et al. 2015. Methane seep ecosystem functions and services from a recently discovered southern California seep. Marine Ecology, 36(S1): 91–108

Guan Hongxiang, Feng Dong, Wu Nengyou, et al. 2016. Methane seepage intensities traced by biomarker patterns in authigenic carbonates from the South China Sea. Organic Geochemistry, 91: 109–119

Guan Hongxiang, Sun Yongge, Zhu Xiaowei, et al. 2013. Factors controlling the types of microbial consortia in cold-seep environments: a molecular and isotopic investigation of authigenic carbonates from the South China Sea. Chemical Geology, 354: 55–64

Haas A, Peckmann J, Elvert M, et al. 2010. Patterns of carbonate authigenesis at the Kouilou pockmarks on the Congo deep-sea fan. Marine Geology, 268(1–4): 129–136

Haeckel M, Suess E, Wallmann K, et al. 2004. Rising methane gas bubbles form massive hydrate layers at the seafloor. Geochimica et Cosmochimica Acta, 68(21): 4335–4345

Han Xiqiu, Suess E, Huang Yongyang, et al. 2008. Jiulong methane reef: microbial mediation of seep carbonates in the South China Sea. Marine Geology, 249(3–4): 243–256

Han Xiqiu, Suess E, Liebetrau V, et al. 2014. Past methane release events and environmental conditions at the upper continental slope of the South China Sea: constraints by seep carbonates. International Journal of Earth Sciences, 103(7): 1873–1887

Han Xiqiu, Yang Kehong, Huang Yongyang. 2013. Origin and nature of cold seep in northeastern Dongsha area, South China Sea: evidence from chimney-like seep carbonates. Chinese Science Bulletin, 58(30): 3689–3697

Himmler T, Birgel D, Bayon G, et al. 2015. Formation of seep carbonates along the Makran convergent margin, northern Arabian Sea and amolecular and isotopic approach to constrain the carbon isotopic composition of parent methane. Chemical Geology, 415: 102–117

Hovland M, Jensen S, Fichler C. 2012. Methane and minor oil macroseep systems-Their complexity and environmental significance. Marine Geology, 332–334: 163–173

Hu Yu, Feng Dong, Liang Qianyong, et al. 2015. Impact of anaerobic oxidation of methane on the geochemical cycle of redox-sensitive elements at cold-seep sites of the northern South China Sea. Deep Sea Research Part II: Topical Studies in Oceanography, 122: 84–94

Huang Yongyang, Suess E, Wu Nengyou. 2008. Methane and Gas Hydrate Geology of the Northern South China Sea: Sino-German Cooperative DO-177 Cruise Report (in Chinese). Beijing: Geological Publishing House

Hutchens E, Gleeson D, McDermott F, et al. 2010. Meter-scale diversity of microbial communities on a weathered pegmatite granite outcrop in the wicklow mountains, ireland; evidence for mineral induced selection. Geomicrobiology Journal, 27(1): 1–14

Hyun S, Bahk J J, Yim U H, et al. 2014. Carbon isotope variations in diploptene for methane hydrate dissociation during the last glacial episode in the Japan Sea/East Sea. Geochemical Journal, 48(3): 287–297

Jensen J B, Kuijpers A, Bennike O, et al. 2002. New geological aspects for freshwater seepage and formation in Eckernförde Bay, western Baltic. Continental Shelf Research, 22(15): 2159–2173

Joye S B, Bowles M W, Samarkin V A, et al. 2010. Biogeochemical signatures and microbial activity of different cold-seep habitats along the Gulf of Mexico deep slope. Deep Sea Research Part II: Topical Studies in Oceanography, 57(21–23): 1990–2001

Judd A G. 2003. The global importance and context of methane escape from the seabed. Geo-Marine Letters, 23(3–4): 147–154

Judd A G, Hovland M, Dimitrov L I, et al. 2002. The geological methane budget at Continental Margins and its influence on climate change. Geofluids, 2(2): 109–126

Kastner M, Kvenvolden K A, Lorenson T D. 1998. Chemistry, isotopic composition, and origin of a methane-hydrogen sulfide hy-

drate at the Cascadia subduction zone. Earth and Planetary Science Letters, 156(3–4): 173–183

Knittel K, Boetius A. 2009. Anaerobic oxidation of methane: progress with an unknown process. Annual Review of Microbiology, 63(1): 311–334

Knittel K, Lösekann T, Boetius A, et al. 2005. Diversity and distribution of methanotrophic archaea at cold seeps. Applied and Environmental Microbiology, 71(1): 467–479

Krumins V, Gehlen M, Arndt S, et al. 2013. Dissolved inorganic carbon and alkalinity fluxes from coastal marine sediments: model estimates for different shelf environments and sensitivity to global change. Biogeosciences, 10(1): 371–398

Li Yiliang, Peacock A D, White D C, et al. 2007. Spatial patterns of bacterial signature biomarkers in marine sediments of the Gulf of Mexico. Chemical Geology, 238(3–4): 168–179

Liebetrau V, Augustin N, Kutterolf S, et al. 2014. Cold-seep-driven carbonate deposits at the Central American forearc: contrasting evolution and timing in escarpment and mound settings. International Journal of Earth Sciences, 103(7): 1845–1872

Lim Y C, Lin S, Yang T F, et al. 2011. Variations of methane induced pyrite formation in the accretionary wedge sediments offshore southwestern Taiwan. Marine and Petroleum Geology, 28(10): 1829–1837

Lin Huiling, Lin C Y, Meyers P A. 2001. Data report: carbonate, organic carbon, and opal concentrations and organic $\delta^{13}C$ values of sediments from sites 1075–1082 and 1084, Southwest Africa margin. In: Wefer G, Berger W H, Richter C, eds. Proceedings of the Ocean Drilling Program Scientific Results

Lin Zhiyong, Sun Xiaoming, Lu Yang, et al. 2016a. Stable isotope patterns of coexisting pyrite and gypsum indicating variable methane flow at a seep site of the Shenhu area, South China Sea. Journal of Asian Earth Sciences, 123: 213–223

Lin Zhiyong, Sun Xiaoming, Peckmann J, et al. 2016b. How sulfate-driven anaerobic oxidation of methane affects the sulfur isotopic composition of pyrite: a SIMS study from the South China Sea. Chemical Geology, 440: 26–41

Lin Qi, Wang Jiasheng, Taladay K, et al. 2016c. Coupled pyrite concentration and sulfur isotopic insight into the paleo sulfate-methane transition zone (SMTZ) in the northern South China Sea. Journal of Asian Earth Sciences, 115: 547–556

Liu Lihua, Shao Haibing, Fu Shaoying, et al. 2016a. Theoretical simulation of the evolution of methane hydrates in the case of Northern South China Sea since the last glacial maximum. Environmental Earth Sciences, 75: 596

Liu Xiao, Xu Tianfu, Tian Hailong, et al. 2016b. Numerical modeling study of mineralization induced by methane cold seep at the sea bottom. Marine and Petroleum Geology, 75: 14–28

Lu Yang, Sun Xiaoming, Lin Zhiyong, et al. 2015. Cold seep status archived in authigenic carbonates: mineralogical and isotopic evidence from Northern South China Sea. Deep Sea Research Part II: Topical Studies in Oceanography, 122: 95–105

Luff R, Greinert J, Wallmann K, et al. 2005. Simulation of long-term feedbacks from authigenic carbonate crust formation at cold vent sites. Chemical Geology, 216(1–2): 157–174

Luff R, Wallmann K. 2003. Fluid flow, methane fluxes, carbonate precipitation and biogeochemical turnover in gas hydrate-bearing sediments at Hydrate Ridge, Cascadia Margin: numerical modeling and mass balances. Geochimica et Cosmochimica Acta, 67(18): 3403–3421

Luff R, Wallmann K, Aloisi G. 2004. Numerical modeling of carbonate crust formation at cold vent sites: significance for fluid and methane budgets and chemosynthetic biological communities. Earth and Planetary Science Letters, 221(1–4): 337–353

Luff R, Wallmann K, Grandel S, et al. 2000. Numerical modeling of benthic processes in the deep Arabian Sea. Deep Sea Research Part II: Topical Studies in Oceanography, 47(14): 3039–3072

Magalhães V H, Pinheiro L M, Ivanov M K, et al. 2012. Formation processes of methane-derived authigenic carbonates from the Gulf of Cadiz. Sedimentary Geology, 243–244: 155–168

Malone M J, Claypool G, Martin J B, et al. 2002. Variable methane fluxes in shallow marine systems over geologic time: the composition and origin of pore waters and authigenic carbonates on the New Jersey shelf. Marine Geology, 189(3–4): 175–196

Martens C S, Albert D B, Alperin M J. 1999. Stable isotope tracing of anaerobic methane oxidation in the gassy sediments of Eckernfoerde Bay, German Baltic Sea. American Journal of Science, 299(7–9): 589–610

Matsumoto R. 2000. Methane hydrate estimates from the chloride and oxygen isotopic anomalies: examples from the Blake Ridge and Nankai trough sediments. Annals of the New York Academy of Sciences, 912: 39–50

Meile C, Koretsky C M, Van Cappellen P. 2001. Quantifying bioirrigation in aquatic sediments: an inverse modeling approach. Limnology and Oceanography, 46(1): 164–177

Ménot G, Bard E. 2010. Geochemical evidence for a large methane release during the last deglaciation from Marmara Sea sediments. Geochimica et Cosmochimica Acta, 74(5): 1537–1550

Meysman F J R, Middelburg J J, Herman P M J, et al. 2003. Reactive transport in surface sediments: I. Model complexity and software quality. Computers & Geosciences, 29(3): 291–300

Nelson H, Thor D R, Sandstrom M W, et al. 1979. Modern biogenic gas-generated craters (sea-floor "pockmarks") on the bering shelf, alaska. Geological Society of America Bulletin, 90(12): 1144–1152

Novikova S A, Shnyukov Y F, Sokol E V, et al. 2015. A methane-derived carbonate build-up at a cold seep on the Crimean slope, north-western Black Sea. Marine Geology, 363: 160–173

Pancost R D, Bouloubassi I, Aloisi G, et al. 2001. Three series of non-isoprenoidal dialkyl glycerol diethers in cold-seep carbonate crusts. Organic Geochemistry, 32(5): 695–707

Paull C K, Ussler W III, Holbrook W S, et al. 2008. Origin of pockmarks and chimney structures on the flanks of the Storegga Slide, offshore Norway. Geo-Marine Letters, 28(1): 43–51

Peckmann J, Gischler E, Oschmann W, et al. 2001. An early carboniferous seep community and hydrocarbon-derived carbonates from the Harz Mountains, Germany. Geology, 29(3): 271–274

Peckmann J, Thiel V. 2004. Carbon cycling at ancient methane-seeps. Chemical Geology, 205(3–4): 443–467

Reed D C, Slomp C P, de Lange G J. 2011. A quantitative reconstruction of organic matter and nutrient diagenesis in Mediterranean Sea sediments over the Holocene. Geochimica et Cosmochimica Acta, 75(19): 5540–5558

Regnier P, Dale A W, Arndt S, et al. 2011. Quantitative analysis of anaerobic oxidation of methane (AOM) in marine sediments: a modeling perspective. Earth-Science Reviews, 106(1–2): 105–130

Roalkvam I, Jorgensen S L, Chen Yifeng, et al. 2011. New insight into stratification of anaerobic methanotrophs in cold seep sediments. FEMS Microbiology Ecology, 78(2): 233–243

Röemer M, Sahling H, Pape T, et al. 2012. Geological control and magnitude of methane ebullition from a high-flux seep area in the Black Sea-the Kerch seep area. Marine Geology, 319–322: 57–74

Rollet N, Logan G A, Kennard J M, et al. 2006. Characterisation and correlation of active hydrocarbon seepage using geophysical data sets: an example from the tropical, carbonate Yampi Shelf, Northwest Australia. Marine and Petroleum Geology, 23(2): 145–164

Sahoo S K, Planavsky N J, Kendall B, et al. 2012. Ocean oxygenation in the wake of the Marinoan glaciation. Nature, 489(7417): 546–549

Sassen R, Roberts H H, Carney R, et al. 2004. Free hydrocarbon gas, gas hydrate, and authigenic minerals in chemosynthetic communities of the northern Gulf of Mexico continental slope: relation to microbial processes. Chemical Geology, 205(3–4): 195–217

Scholz F, Hensen C, Noffke A, et al. 2011. Early diagenesis of redox-sensitive trace metals in the Peru upwelling area-response to ENSO-related oxygen fluctuations in the water column. Geochimica et Cosmochimica Acta, 75(22): 7257–7276

Schouten S, Breteler W C M K, Blokker P, et al. 1998. Biosynthetic effects on the stable carbon isotopic compositions of algal lipids:

implications for deciphering the carbon isotopic biomarker record. Geochimica et Cosmochimica Acta, 62(8): 1397–1406

Sivan O, Schrag D P, Murray R W. 2007. Rates of methanogenesis and methanotrophy in deep-sea sediments. Geobiology, 5(2): 141–151

Stadnitskaia A, Baas M, Ivanov M K, et al. 2003. Novel archaeal macrocyclic diether core membrane lipids in a methane-derived carbonate crust from a mud volcano in the Sorokin Trough, NE Black Sea. Archaea, 1(3): 165–173

Stadnitskaia A, Muyzer G, Abbas B, et al. 2005. Biomarker and 16S rDNA evidence for anaerobic oxidation of methane and related carbonate precipitation in deep-sea mud volcanoes of the Sorokin Trough, Black Sea. Marine Geology, 217(1–2): 67–96

Suess E. 2005. RV Sonne cruise report SO 177, Sino-German cooperative project, south China Sea continental margin: geological methane budget and environmental effects of methane emissions and gashydrates. IFM-GEOMAR Reports

Suess E. 2014. Marine cold seeps and their manifestations: geological control, biogeochemical criteria and environmental conditions. International Journal of Earth Sciences, 103(7): 1889–1916

Talukder A R, Ross A, Crooke E, et al. 2013. Natural hydrocarbon seepage on the continental slope to the east of Mississippi Canyon in the northern Gulf of Mexico. Geochemistry, Geophysics, Geosystems, 14(6): 1940–1956

Tong Hongpeng, Feng Dong, Cheng Hai, et al. 2013. Authigenic carbonates from seeps on the northern continental slope of the South China Sea: new insights into fluid sources and geochronology. Marine and Petroleum Geology, 43: 260–271

Treude T, Niggemann J, Kallmeyer J, et al. 2005. Anaerobic oxidation of methane and sulfate reduction along the Chilean continental margin. Geochimica et Cosmochimica Acta, 69(11): 2767–2779

Treude T, Orphan V, Knittel K, et al. 2007. Consumption of methane and CO_2 by methanotrophic microbial mats from gas seeps of the anoxic Black Sea. Applied and Environmental Microbiology, 73(7): 2271–2283

van Dongen B E, Roberts A P, Schouten S, et al. 2007. Formation of iron sulfide nodules during anaerobic oxidation of methane. Geochimica et Cosmochimica Acta, 71(21): 5155–5167

Vanneste H, James R H, Kelly-Gerreyn B A, et al. 2013. Authigenic barite records of methane seepage at the Carlos Ribeiro mud volcano (Gulf of Cadiz). Chemical Geology, 354: 42–54

Wallmann K, Aloisi G, Haeckel M, et al. 2006. Kinetics of organic matter degradation, microbial methane generation, and gas hydrate formation in anoxic marine sediments. Geochimica et Cosmochimica Acta, 70(15): 3905–3927

Wang Shuhong, Yan Bin, Yan Wen. 2013. Tracing seafloor methane emissions with benthic foraminifera in the Baiyun Sag of the northern South China Sea. Environmental Earth Sciences, 70(3): 1143–1150

Whiticar M J. 1999. Carbon and hydrogen isotope systematics of bacterial formation and oxidation of methane. Chemical Geology, 161(1–3): 291–314

Yin P, Berné S, Vagner P, et al. 2003. Mud volcanoes at the shelf margin of the East China Sea. Marine Geology, 194(3–4): 135–149